ACS Macro Letters

Letter

pubs.acs.org/macroletters

Fine Tuning Surface Energy of Poly(3-hexylthiophene) by Heteroatom Modification of the Alkyl Side Chains

Jenna B. Howard, Sangtaik Noh, Alejandra E. Beier, and Barry C. Thompson*

Department of Chemistry, Loker Hydrocarbon Research Institute, University of Southern California, Los Angeles, California 90089-1661, United States

Supporting Information

ABSTRACT: Recent work has pointed to polymer miscibility and surface energy as key figures of merit in the formation of organic alloys and synergistic behavior between components in ternary blend solar cells. Here, we present a simple model system and first report of poly(3-hexylthiophene)-based random copolymers featuring either a semifluoroalkyl (P3HT-*co*-FHT) or oligoether (P3HT-*co*-MET) side chain, prepared via Stille polycondensation. Water drop contact angle measurements demonstrated that P3HT-*co*-FHT polymers reached a minimum surface energy of 14.2 mN/m at 50% composition of comonomers, while in contrast, P3HT-*co*-MET polymers increased as high as 27.0 mN/m at 50% composition, compared to P3HT at 19.9 mN/m. Importantly, the surface energy of the copolymers was found to vary regularly with comonomer composition and exhibited fine-tuning. Optical and electronic properties of the polymers are found to be composition independent as determined by UV−vis and CV measurements; HOMO energy levels ranged from 5.25 to 5.30 eV; and optical band gaps all measured 1.9 eV. Following this model, surface energy modification of state-of-the-art polymers, without altering desirable electronic and optical properties, is proposed as a useful tool in identifying and exploiting more alloying polymer pairs for ternary blend solar cells.

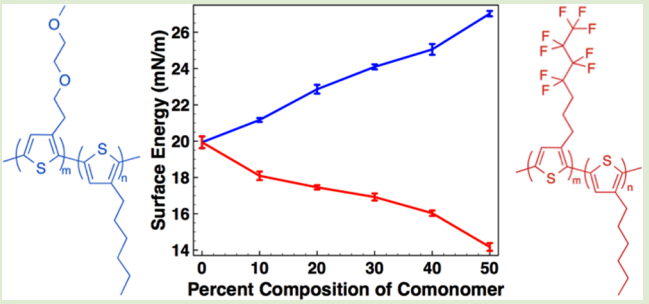

Conjugated polymers are promising materials for low-cost, solution processable devices such as organic solar cells and field effect transistors.[1] The structure−function relationships of conjugated polymers have been widely explored to elucidate high performing donor materials for organic photovoltaic (OPV) applications. Systematic modification of the polymer's primary structure to tune HOMO/LUMO levels and optical band gaps is well understood through considering donor−acceptor push−pull effects and chain packing.[2] To date, many features such as alternating,[3−5] random,[6,7] and semirandom donor−acceptor structures,[8,9] backbone planarity,[10] and side chains[5,6,11,12] have been tools for manipulating polymer properties toward optimized short-circuit currents (J_{SC}) and open-circuit voltages (V_{OC}).[13,14] Additionally, several studies have focused on how primary polymer structure can influence polymer−fullerene interactions in binary bulk heterojunction (BHJ) solar cells for optimized charge separation and transport.[15] Specific arrangements and lengths of side chains have also been utilized to control fullerene miscibility and intercalation.[16−18] Significant progress in this field of research has pushed single-layer BHJ solar cells with state-of-the-art donor materials to record efficiencies in the range of 8−10%.[19]

An emerging class of devices, known as ternary blend solar cells, utilizes either two acceptors and one donor (D:A1$_x$A2$_{(1-x)}$)[20] or two donors with one acceptor (D1$_x$D2$_{(1-x)}$:A),[21] where x represents the composition range from 0 to 1. More typically, ternary blends with two donors have been found to benefit from enhanced J_{SC} due to complementary absorption and composition-dependent V_{OC} derived from the synergistic donor materials.[22] Recently, we reported that polymer compatibility between two polymer donor materials is a significant factor in the formation of previously described organic alloys, leading to an intermediate V_{OC} rather than a lower, pinned value that would suggest hole trapping in the highest lying HOMO.[23] The organic alloy model suggests that two donors or acceptors experience an averaging of frontier orbitals when there is miscibility between the materials. Specifically, the random-copolymer effect[24] supports polymer pairs that demonstrated alloying behavior, which are random or semirandom, based on common comonomers, and exhibit cocrystallization behavior. More generally, similar surface energy was attributed as a key figure of merit for predicting pairs of polymers that may be used synergistically together in a ternary blend system. In the case of dissimilar surface energies, devices fabricated with blends containing two donors, up to 95% composition of the lower-lying HOMO polymer, showed pinning to the V_{OC} corresponding to that of the other higher-lying HOMO polymer, whereas devices incorporating two donor materials with similar surface energies showed a compositionally

Received: May 18, 2015
Accepted: June 22, 2015
Published: June 23, 2015

DOI: 10.1021/acsmacrolett.5b00328
ACS Macro Lett. 2015, 4, 725−730

Scheme 1. Synthesis of (a) Comonomer 4 and (b) Comonomer 7

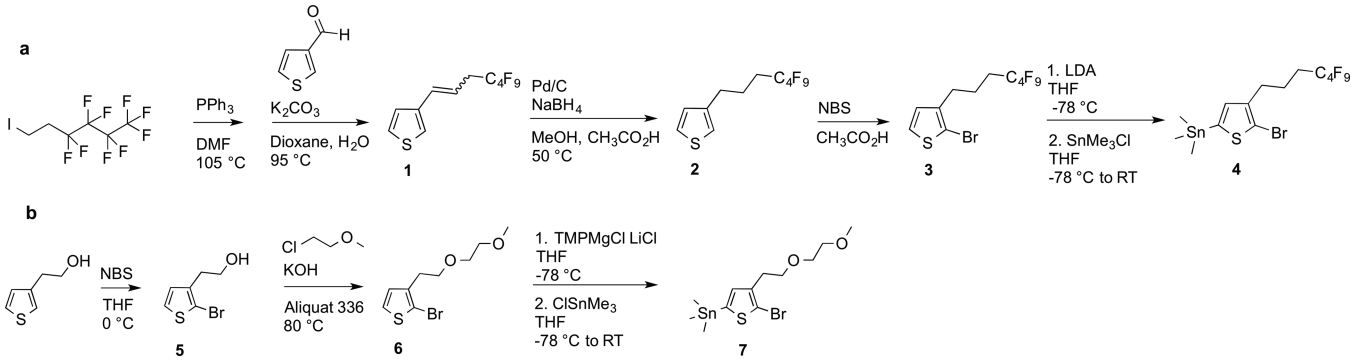

Scheme 2. Stille Polycondensation of Comonomers

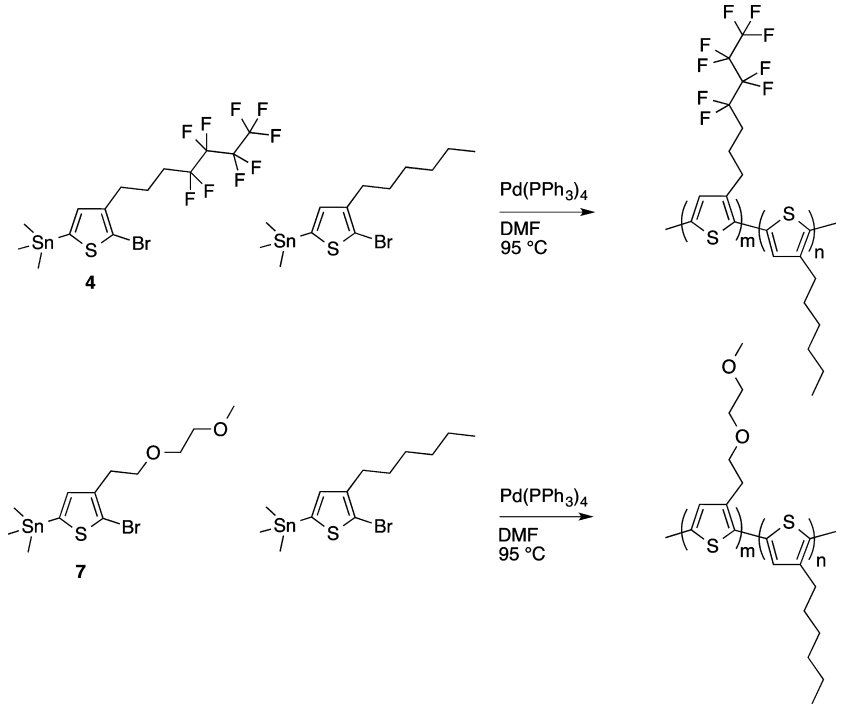

dependent V_{OC}.[23] Surface energy can be correlated with a material's Flory–Huggins interaction parameter (χ) which is used to characterize polymer–polymer interactions.[25] Several recent studies have included surface energy measurements and indicate it as a strong predictor of material compatibility in organic photovoltaics.[26−34]

Currently, features of conjugated polymer primary structure and their influence on surface energy remain widely unexplored, even though such information may be a useful tool for predicting favorable candidates for binary and especially ternary blend solar cells. Moreover, a modular method for tuning the surface energy of existing state-of-the-art conjugated polymers without altering their desirable optical and electronic properties may enable more pairing options for ternary blends from well-known polymers with complementary absorption profiles and different HOMO levels. While a handful of successful ternary blend systems have been identified,[20,21,35−37] little is known about the influence of primary structure on cooperative effects in these materials, which has prompted the need for a better understanding and control of polymer–polymer interactions and blending.[20−22]

Here we present a simple chemical modification of the alkyl side chains of 3-alkylthiophene monomers toward a new family of random copolymers with fine-tuned surface energy profiles. Poly(3-hexylthiophene) (P3HT) is a well-known conjugated polymer used in BHJ solar cells, with a simple primary structure that may be manipulated for studying surface energy as an isolated variable. With the goal of maintaining the optical and electronic properties of P3HT, the alkyl side chains were identified as a point of modification toward tuning surface energy. Previous studies have established that small incorporation of a comonomer into a regioregular copolymer can fine-tune specific polymer properties while maintaining the desirable properties of P3HT.[6,8,9] In the present case, the alkyl chains were modified to contain varying amounts of fluorine or oxygen atoms to induce hydrophobic or hydrophilic interactions, respectively, and directly control the surface energy. Precise control of the comonomer compositions allows for tuning of the surface energy. Modification of the alkyl chain was executed with a spacer of at least two carbons in length to diminish any electronic effects from the heteroatoms on the conjugated backbone.

DOI: 10.1021/acsmacrolett.5b00328
ACS Macro Lett. 2015, 4, 725−730

Table 1. Molecular Weights (PDI), Electrochemical HOMO Values, Optical Band Gaps, and SCLC Mobilities of P3HT, P3HT-*co*-FHT, and P3HT-*co*-MET Polymers

polymer	M_n (kDa) (PDI)[a]	HOMO (eV) (solution)[b]	HOMO (eV) (film)[c]	E_g (eV)[d]	μ_h ($cm^2\ V^{-1}\ s^{-1}$)[e]	T_m; T_c (°C)[f]
P3HT	25.7 (2.6)	5.25	5.24	1.9	8.10×10^{-5}	221; 186
$P3HT_{90}$-*co*-FHT_{10}	41.8 (1.7)	5.30	5.30	1.9	1.02×10^{-5}	221; 187
$P3HT_{80}$-*co*-FHT_{20}	42.9 (1.7)	5.29	5.30	1.9	7.98×10^{-5}	231; 205
$P3HT_{70}$-*co*-FHT_{30}	40.9 (1.84)	5.30	5.28	1.9	2.86×10^{-5}	236; 216
$P3HT_{60}$-*co*-FHT_{40}	29.1 (1.78)	5.30	5.27	1.9	1.46×10^{-5}	233; 213
$P3HT_{50}$-*co*-FHT_{50}	-	5.30	5.30	1.9	5.45×10^{-7}	239; 221
$P3HT_{90}$-*co*-MET_{10}	23.6 (2.0)	5.29	5.29	1.9	3.45×10^{-5}	- ; -
$P3HT_{80}$-*co*-MET_{20}	21.0 (2.0)	5.29	5.29	1.9	1.35×10^{-4}	- ; 109
$P3HT_{70}$-*co*-MET_{30}	14.5 (2.3)	5.30	5.27	1.9	2.38×10^{-5}	- ; 124
$P3HT_{60}$-*co*-MET_{40}	9.9 (1.6)	5.29	5.25	1.9	1.78×10^{-4}	- ; 99
$P3HT_{50}$-*co*-MET_{50}	8.5 (1.4)	5.28	5.29	1.9	1.51×10^{-4}	-; 115

[a]Determined by SEC with polystyrene standards and *o*-DCB eluent. $P3HT_{50}$-*co*-FHT_{50} was not sufficiently soluble in *o*-DCB at the required concentration for analysis. [b]Cyclic voltammetry (vs Fc/Fc^+) in chloroform, 0.1 M $TBABF_4$. [c]Cyclic voltammetry (vs Fc/Fc^+) in acetonitrile, 0.1 M $TBAPF_6$. [d]Calculated from the absorption band edge in thin films, $E_g = 1240/\lambda_{edge}$. [e]Measured for neat, as-cast polymer films. [f]The absence of a T_m or T_c is indicated by "-".

Synthesis of comonomer, **4** (Scheme 1a), was achieved from modified literature procedures,[38] via a Wittig coupling, followed by hydrogenation, electrophilic bromination, and finally a lithiation and subsequent stannylation. Comonomer **7** (Scheme 1b) was also prepared following modifications of previous literature procedures[39] by an electrophilic bromination followed by a Williamson-ether synthesis. Intermediate **6** could not be stannylated via the 5-lithiated intermediate, which led to inseparable isomers, but rather a 5-magnesiated intermediate generated from the Knochel–Hauser base.[40,41] To the best of our knowledge, this is the first report of both of the final monomers with the 5-position functionalized with a trimethyl tin group. To date, the previously reported monomer precursors **3** and **6** and similar monomer structures with longer oligoether or semi or perfluoroalkyl chains have been used in oligomer syntheses,[38,42] GRIM,[43,44] oxidative,[45] or electropolymerizations[46−48] to form homopolymers. Comonomers **4** and **7** were subsequently copolymerized in 10−50% feed ratio with 2-bromo-3-hexyl-5-(trimethylstannyl) thiophene under Stille polycondensation conditions (Scheme 2, M_n and PDI reported in Table 1). Proton NMR spectra of the polymers support the feed ratios and composition of the comonomers (Figures S1 and S2, Supporting Information). Polymers containing a semifluoro alkyl chain are designated as $P3HT_x$-*co*-FHT_{100-x} with x representing percent composition of 3-hexylthiophene. Likewise, polymers containing a methoxy–ethoxy–ethyl chain are designated as $P3HT_x$-*co*-MET_{100-x}. This is the first report of regioregular, random P3HT-*co*-FHT. While Bilkay and co-workers[44] previously reported P3HT-*co*-MET via GRIM with different monomer feed ratios, this is the first report of P3HT-*co*-MET via Stille polycondensation, which is made possible by successful stannylation to prepare monomer **7**. P3HT-*co*-FHT polymers exhibited decreasing solubility in *o*-DCB with increasing content of the comonomer, to the extent that $P3HT_{50}$-*co*-FHT_{50} was not sufficiently soluble for GPC analysis. For this reason, we chose only to compare up to 50% composition for both polymer families.

Critically, surface energies of the polymers were determined using a contact angle goniometer. Contact angle measurements of water on pristine, as-cast polymer films revealed that P3HT-*co*-FHT polymer surface energy steadily decreases with increasing content of the semifluoro alkylthiophene monomer (Figure 1a). Incorporation of the comonomer up to 50% resulted in surface energy as low as 14.2 mN/m compared to P3HT at 19.9 mN/m for as-cast blends. This trend is also observed in thermally annealed polymer films (Figure 1b); however, P3HT-*co*-FHT polymers with 10−30% FHT composition appear to have roughly the same surface energy as P3HT. This is perhaps due to a change in content of fluoro side chains at the polymer film surface relative to the bulk after thermal annealing. In contrast, polymers containing methoxy–ethoxy–ethylene side chains gradually increased in surface energy, up to 27.0 and 26.3 mN/m at 50% comonomer composition for as-cast and annealed films, respectively (Figure 1). A direct comparison of all surface energy data is also presented in a single plot (Figure S3, Supporting Information).

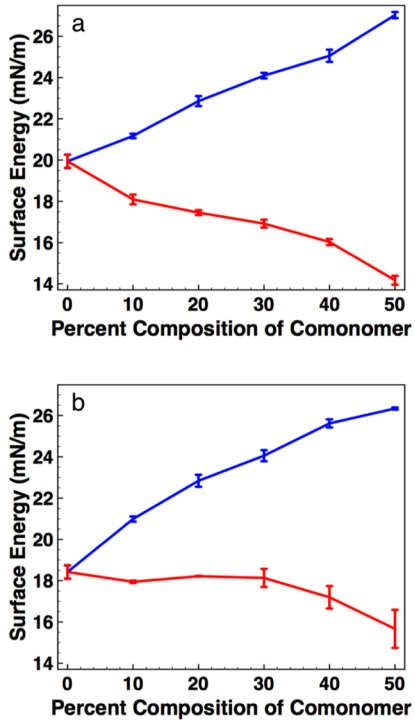

Figure 1. Surface energy of P3HT-*co*-MET (blue) and P3HT-*co*-FHT (red) polymers measured from (a) as-cast thin films and (b) thermally annealed thin films. P3HT-*co*-MET and P3HT films were annealed at 100 °C, and P3HT-*co*-FHT films were annealed at 150 °C.

DOI: 10.1021/acsmacrolett.5b00328
ACS Macro Lett. 2015, 4, 725−730

Surface energy calculations based on a two-liquid approach, using water and glycerol, with the Wu model were also completed, and the data are available in the Supporting Information (Figure S4). While our previous research and others have utilized the Wu model,[23,26,29−31] here we choose to present the one-liquid method due to previously reported large variations in surface energy measurements with the two-liquid method when the pair of testing liquids does not include a completely dispersive and compatible solvent that can be used consistently for all samples.[49,50] Many material studies of surface energy utilize diiodomethane as the dispersive solvent, which poses solubilizing problems during the measurement of the solid conjugated polymer films. Previous measurements of conjugated polymers, including our own, have opted to use glycerol as the dispersive solvent for the two-liquid method; however, glycerol may pose a solubilizing problem for the P3HT-*co*-MET polymer family. As such, the one-liquid method with water is found to be most applicable to this study.

While the desired effect on surface energy was clearly demonstrated, importantly the optical and electronic properties were found to be unaffected by side chain identity and composition. The optical properties of the resulting polymers were characterized by UV−vis, specifically to explore effects of comonomer composition on polymer band gap and absorption coefficient in films cast from chloroform. Absorption profiles for both P3HT-*co*-MET and P3HT-*co*-FHT families are P3HT-like, with lower absorption coefficients for both as-cast (Figure 2) and annealed films (Figure S5, Supporting Information) relative to P3HT. Absorption coefficients for all P3HT-*co*-FHT polymers increase, and vibronic shoulders are more prominent after thermal annealing (Figure S5a, Supporting Information). P3HT-*co*-MET polymer absorption coefficients remain the same after annealing, with the exception of $P3HT_{50}$-*co*-MET_{50}, which decreases slightly. All P3HT-*co*-MET polymer absorption maxima blue shift between 20 and 30 nm after annealing. Strikingly, some polymers, such as $P3HT_{60}$-*co*-MET_{40} and $P3HT_{50}$-*co*-MET_{50}, bear prominent vibronic shoulders in the as-cast blends where others do not (Figure 2b).

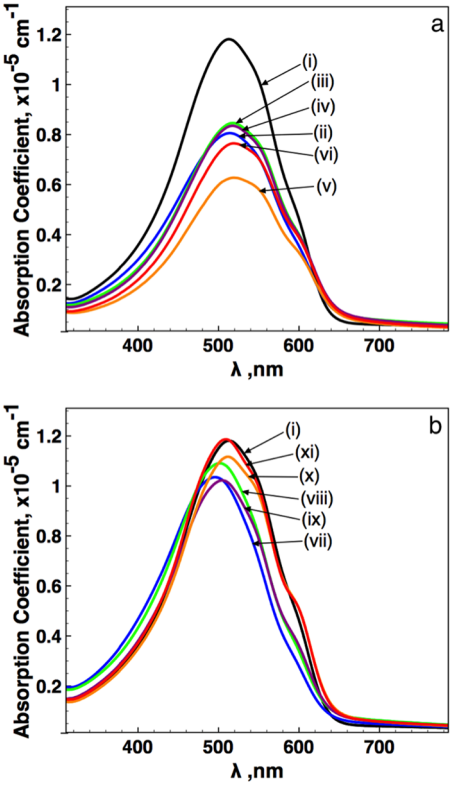

Figure 2. Absorption profiles of (a) as-cast P3HT-*co*-FHT and (b) as-cast P3HT-*co*-MET films spin coated from chloroform: (i) P3HT, (ii) $P3HT_{90}$-*co*-FHT_{10}, (iii) $P3HT_{80}$-*co*-FHT_{20}, (iv) $P3HT_{70}$-*co*-FHT_{30}, (v) $P3HT_{60}$-*co*-FHT_{40}, (vi) $P3HT_{50}$-*co*-FHT_{50}, (vii) $P3HT_{90}$-*co*-MET_{10}, (viii) $P3HT_{80}$-*co*-MET_{20}, (ix) $P3HT_{70}$-*co*-MET_{30}, (x) $P3HT_{60}$-*co*-MET_{40}, and (xi) $P3HT_{50}$-*co*-MET_{50}.

The absorption coefficient decreases could be explained given the volume of the polymeric material, as polymers containing a higher content of the heteroatom chains (both of which are seven atoms in length) spatially contain less chromophore than that of P3HT with six-carbon alkyl chains. Alternatively, the presence of heteroatom alkyl chains may induce varied packing compared to that of P3HT, which would be reflected in the absorption profiles and maxima.[46] The differences in absorption coefficient and maxima were investigated by GIXRD and are discussed later. $P3HT_{60}$-*co*-MET_{40} and $P3HT_{50}$-*co*-MET_{50} polymers feature vibronic shoulders in as-cast blends, similar to what is seen for P3HT films after annealing (Figure 2b), suggesting self-organization within the films without the need for thermal or solvent vapor annealing. Optical band gaps, derived from absorption onset of films, of all polymers are 1.9 eV (Table 1), unchanged by the alkyl chain modification.

Additionally, CV was completed for comparison of HOMO energy levels of the polymers (Table 1). Both solution and film CVs were examined; all P3HT-*co*-FHT and P3HT-*co*-MET polymers measured between 5.25 and 5.30 eV, with no observable trend within each family. Analysis of optical and electronic data suggests that both families of polymers exhibit band gaps, absorption profiles, and solid-state HOMO levels that are virtually identical to that of P3HT. These P3HT-like properties were likely maintained by the incorporation of a carbon spacer to physically decouple the heteroatoms from the backbone conjugation.

As previously mentioned, the UV−vis study of the P3HT-*co*-FHT and P3HT-*co*-MET polymers revealed variations in absorption coefficient and maxima suggesting differences in the polymer chain packing relative to P3HT. For a full comparison, all P3HT-*co*-MET and P3HT-*co*-FHT polymers were studied using GIXRD to gain insight into these differences. The GIXRD *d*-spacings of P3HT-*co*-FHT as-cast and annealed films indicate a larger spacing in lamellar packing as the content of the FHT comonomer is increased (Figure 3a and Figure S7a, Supporting Information), and the intensity of all signals increases after thermal annealing. Interestingly, the *d*-spacings for P3HT-*co*-MET polymers are similar to that of P3HT for both as-cast and annealed films (Figure 3b and Figure S7b, Supporting Information), while the intensity of the signal increases with higher contents of the comonomer; all signals also increase after thermal annealing.

The larger spacing in lamellar packing of P3HT-*co*-FHT polymers is consistent with our hypothesis that the side chains spatially encompass greater volumes, consistent with a lower absorption coefficient relative to P3HT. However, as-cast P3HT-*co*-MET polymer films have the opposite trend compared to P3HT-*co*-FHT polymers, where the absorption coefficient increases with increasing MET monomer content. By comparison, the MET side chain lacks hydrogen atoms relative to an alkyl or semifluoro alkyl chain, which may

DOI: 10.1021/acsmacrolett.5b00328
ACS Macro Lett. 2015, 4, 725−730

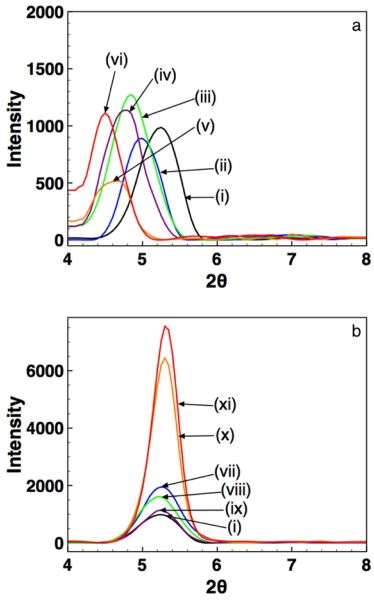

Figure 3. GIXRD data of (a) P3HT-*co*-FHT and (b)P3HT-*co*-MET annealed films: (i) P3HT, (ii) $P3HT_{90}$-*co*-FHT_{10}, (iii) $P3HT_{80}$-*co*-FHT_{20}, (iv) $P3HT_{70}$-*co*-FHT_{30}, (v) $P3HT_{60}$-*co*-FHT_{40}, (vi) $P3HT_{50}$-*co*-FHT_{50}, (vii) $P3HT_{90}$-*co*-MET_{10}, (viii) $P3HT_{80}$-*co*-MET_{20}, (ix) $P3HT_{70}$-*co*-MET_{30}, (x) $P3HT_{60}$-*co*-MET_{40}, and (xi) $P3HT_{50}$-*co*-MET_{50}.

counteract the longer chain length and allow for tighter packing, which is supported by the greater intensity of the GIXRD peaks as MET content increases. GIXRD data considered together with the observed blue-shift in annealed films indicate that P3HT-*co*-MET polymers may have some unusual packing which may be responsible for absorption coefficient and absorption maxima differences. Additionally, hole mobilities measured by SCLC were slightly higher for $P3HT_{60}$-*co*-MET_{40} and $P3HT_{50}$-*co*-MET_{50} compared to P3HT in as-cast films (Table 1), reflecting the higher level of crystallinity.

Analysis of the UV−vis absorption profiles and GIXRD data of annealed films also suggests differences in thermal transitions that were further explored by DSC. Thermally annealed films (100 °C) of P3HT-*co*-MET polymers have a blue-shifted absorption maxima and vibronic shoulder (Figure S5b, Supporting Information), and GIXRD measurements indicate a greater degree of crystallinity of each annealed polymer film compared to P3HT (Figure 3b). In contrast, P3HT-*co*-FHT polymers exhibited vibronic shoulders and increased crystallinities comparable to P3HT only after thermal annealing at 150 °C (Figure S5a, Supporting Information). The milder thermal annealing conditions of P3HT-*co*-MET required to enhance film crystallinity, compared to P3HT-*co*-FHT polymers, suggest a difference in thermal transitions. A DSC study indicated that the P3HT-*co*-MET polymer family has lower temperature thermal transitions, and P3HT-*co*-FHT polymers have a higher transition, compared to P3HT (Table 1, Figure S29−Figure S38, Supporting Information). These findings are consistent with previously reported thermal behavior of 3-alkylthiophene homopolymers featuring oligo ether[51] or semi fluoro alkyl side chains.[52,53]

Additionally, photoluminescence spectra of selected samples were obtained (Figure S6, Supporting Information) for further comparison. Spectra of P3HT-*co*-FHT polymers have the same profile as P3HT and are observed to increase in intensity with increasing content of comonomer, suggesting a decrease in nonradiative quenching pathways. We attribute the decrease to the larger lamellar spacings of the polymer chains observed in GIXRD of P3HT-*co*-FHT polymers with increasing comonomer content. Interestingly, P3HT-*co*-MET polymers are less emissive than P3HT in as-cast films, indicating higher quenching with the comonomer present. Higher quenching in these films may be consistent with our hypothesis that these polymers can pack tighter than P3HT. Moreover, the annealed film PL spectra of P3HT-*co*-MET polymers exhibit a blue shift, consistent with the UV−vis measurements.

In summary, we have demonstrated that simple chemical modification of monomer alkyl side chains and direct control of their overall composition in conjugated copolymers is an effective method for the fine-tuning of surface energy while maintaining optical and electronic properties. This is the first report of a family of conjugated polymers with a tuned and composition-dependent surface energy profile. The synthetic approaches employed here allow for the preparation of newly reported stannylated monomers and random copolymers, via Stille polycondensation. On the basis of these results, we predict that incorporation of varying amounts of fluorine or oxygen atoms in the alkyl side chains of other well-known conjugated polymers will be an effective tool for modifying surface energies, polymer compatibility, and engendering alloy formation for the further investigation and exploitation of ternary blend organic solar cells.

■ ASSOCIATED CONTENT

Supporting Information

Syntheses of monomer and polymers, ^{13}C and ^{1}H NMR spectra, UV−vis spectra, PL spectra, GIXRD data, Wu model surface energy, DSC, and CV traces. The Supporting Information is available free of charge on the ACS Publications website at DOI: 10.1021/acsmacrolett.5b00328.

■ AUTHOR INFORMATION

Corresponding Author

*E-mail: barrycth@usc.edu.

Notes

The authors declare no competing financial interest.

■ ACKNOWLEDGMENTS

This work is supported by the National Science Foundation (CBET Energy for Sustainability) CBET-1436875. We would like to thank Dr. Malancha Gupta and Scott Siedel for very generously providing training and use of their Rame-Hart Goniometer.

■ REFERENCES

(1) Thompson, B. C.; Fréchet, J. M. J. *Angew. Chem., Int. Ed.* **2008**, *47*, 58−77.
(2) Kroon, R.; Lenes, M.; Hummelen, J. C.; Blom, P. W. M.; de Boer, B. *Polym. Rev.* **2008**, *48*, 531−582.
(3) Chu, T.-Y.; Lu, J.; Beaupré, S.; Zhang, Y.; Pouliot, J.-R.; Wakim, S.; Zhou, J.; Leclerc, M.; Li, Z.; Ding, J.; Tao, Y. *J. Am. Chem. Soc.* **2011**, *133*, 4250−4253.
(4) Park, S. H.; Roy, A.; Beaupré, S.; Cho, S.; Coates, N.; Moon, J. S.; Moses, D.; Leclerc, M.; Lee, K.; Heeger, A. J. *Nat. Photonics* **2009**, *3*, 297−302.
(5) Chen, H.-Y.; Hou, J.; Zhang, S.; Liang, Y.; Yang, G.; Yang, Y.; Yu, L.; Wu, Y.; Li, G. *Nat. Photonics* **2009**, *3*, 649−653.

DOI: 10.1021/acsmacrolett.5b00328
ACS Macro Lett. 2015, 4, 725−730

(6) Burkhart, B.; Khlyabich, P. P.; Thompson, B. C. *Macromolecules* **2012**, *45*, 3740−3748.
(7) Kang, T. E.; Kim, K.-H.; Kim, B. J. *J. Mater. Chem. A* **2014**, *2*, 15252−15267.
(8) Khlyabich, P. P.; Burkhart, B.; Ng, C. F.; Thompson, B. C. *Macromolecules* **2011**, *44*, 5079−5084.
(9) Burkhart, B.; Khlyabich, P. P.; Cakir Canak, T.; LaJoie, T. W.; Thompson, B. C. *Macromolecules* **2011**, *44*, 1242−1246.
(10) Roncali, J. *Chem. Rev.* **1997**, *97*, 173−206.
(11) Mei, J.; Bao, Z. *Chem. Mater.* **2014**, *26*, 604−615.
(12) Thompson, B. C.; Kim, B. J.; Kavulak, D. F.; Sivula, K.; Mauldin, C.; Fréchet, J. M. J. *Macromolecules* **2007**, *40*, 7425−7428.
(13) Beaujuge, P. M.; Fréchet, J. M. J. *J. Am. Chem. Soc.* **2011**, *133*, 20009−20029.
(14) Cheng, Y.-J.; Yang, S.-H.; Hsu, C.-S. *Chem. Rev.* **2009**, *109*, 5868−5923.
(15) Huang, Y.; Kramer, E. J.; Heeger, A. J.; Bazan, G. C. *Chem. Rev.* **2014**, *114*, 7006−7043.
(16) Poelking, C.; Cho, E.; Malafeev, A.; Ivanov, V.; Kremer, K.; Risko, C.; Brédas, J.-L.; Andrienko, D. *J. Phys. Chem. C* **2013**, *117*, 1633−1640.
(17) Cates, N. C.; Gysel, R.; Beiley, Z.; Miller, C. E.; Toney, M. F.; Heeney, M.; McCulloch, I.; McGehee, M. D. *Nano Lett.* **2009**, *9*, 4153−4157.
(18) Lee, C.-K.; Pao, C.-W. *J. Phys. Chem. C* **2012**, *116*, 12455−12461.
(19) Scharber, M. C.; Sariciftci, N. S. *Prog. Polym. Sci.* **2013**, *38*, 1929−1940.
(20) Khlyabich, P. P.; Burkhart, B.; Thompson, B. C. *J. Am. Chem. Soc.* **2011**, *133*, 14534−14537.
(21) Khlyabich, P. P.; Burkhart, B.; Thompson, B. C. *J. Am. Chem. Soc.* **2012**, *134*, 9074−9077.
(22) Street, R. A.; Davies, D.; Khlyabich, P. P.; Burkhart, B.; Thompson, B. C. *J. Am. Chem. Soc.* **2013**, *135*, 986−989.
(23) Khlyabich, P. P.; Rudenko, A. E.; Street, R. A.; Thompson, B. C. *ACS Appl. Mater. Interfaces* **2014**, *6*, 9913−9919.
(24) De Wit, J.; van Ekenstein, G. A.; Polushkin, E.; Korhonen, J.; Ruokolainen, J.; ten Brinke, G. *Macromolecules* **2009**, *42*, 2009−2014.
(25) Sperling, L. H. *Introduction to Physical Polymer Science*, 4th ed.; Wiley-Interscience: New York, 2006.
(26) Huang, J.-H.; Hsiao, Y.-S.; Richard, E.; Chen, C.-C.; Chen, P.; Li, G.; Chu, C.-W.; Yang, Y. *Appl. Phys. Lett.* **2013**, *103*, 043304.
(27) Honda, S.; Ohkita, H.; Benten, H.; Ito, S. *Adv. Energy Mater.* **2011**, *1*, 588−598.
(28) Xu, H.; Ohkita, H.; Hirata, T.; Benten, H.; Ito, S. *Polymer* **2014**, *55*, 2856−2860.
(29) Wang, Y.; Benten, H.; Ohara, S.; Kawamura, D.; Ohkita, H.; Ito, S. *ACS Appl. Mater. Interfaces* **2014**, *6*, 14108−14115.
(30) Sun, Y.; Chien, S.-C.; Yip, H.-L.; Chen, K.-S.; Zhang, Y.; Davies, J. A.; Chen, F.-C.; Lin, B.; Jen, A. K.-Y. *J. Mater. Chem.* **2012**, *22*, 5587.
(31) Kang, H.; Kim, K.-H.; Choi, J.; Lee, C.; Kim, B. J. *ACS Macro Lett.* **2014**, *3*, 1009−1014.
(32) Wang, G.; Jiu, T.; Sun, C.; Li, J.; Li, P.; Lu, F.; Fang, J. *ACS Appl. Mater. Interfaces* **2014**, *6*, 833−838.
(33) Bulliard, X.; Ihn, S.-G.; Yun, S.; Kim, Y.; Choi, D.; Choi, J.-Y.; Kim, M.; Sim, M.; Park, J.-H.; Choi, W.; Cho, K. *Adv. Funct. Mater.* **2010**, *20*, 4381−4387.
(34) Yoon, Y.; Kim, H. J.; Cho, C.-H.; Kim, S.; Son, H. J.; Ko, M.-J.; Kim, H.; Lee, D.-K.; Kim, J. Y.; Lee, W.; Kim, B. J.; Kim, B. *ACS Appl. Mater. Interfaces* **2014**, *6*, 333−339.
(35) Yang, Y. (Michael); Chen, W.; Dou, L.; Chang, W.-H.; Duan, H.-S.; Bob, B.; Li, G.; Yang, Y. *Nat. Photonics* **2015**, *9*, 190−198.
(36) Yang, L.; Zhou, H.; Price, S. C.; You, W. *J. Am. Chem. Soc.* **2012**, *134*, 5432−5435.
(37) Lu, L.; Xu, T.; Chen, W.; Landry, E. S.; Yu, L. *Nat. Photonics* **2014**, *8*, 716−722.
(38) Tanba, S.; Sugie, A.; Masuda, N.; Monguchi, D.; Koumura, N.; Hara, K.; Mori, A. *Heterocycles* **2010**, *82*, 505−529.
(39) Costanzo, P. J.; Stokes, K. K. *Macromolecules* **2002**, *35*, 6804−6810.
(40) Khlyabich, P. P.; Rudenko, A. E.; Thompson, B. C. *J. Polym. Sci., Part A: Polym. Chem.* **2014**, *52*, 1055−1058.
(41) Krasovskiy, A.; Krasovskaya, V.; Knochel, P. *Angew. Chem., Int. Ed.* **2006**, *45*, 2958−2961.
(42) Tanaka, S.; Tamba, S.; Tanaka, D.; Sugie, A.; Mori, A. *J. Am. Chem. Soc.* **2011**, *133*, 16734−16737.
(43) Shao, M.; He, Y.; Hong, K.; Rouleau, C. M.; Geohegan, D. B.; Xiao, K. *Polym. Chem.* **2013**, *4*, 5270−5274.
(44) Bilkay, T.; Schulze, K.; Egorov-Brening, T.; Bohn, A.; Janietz, S. *Macromol. Chem. Phys.* **2012**, *213*, 1970−1978.
(45) Hong, X.; Tyson, J. C.; Middlecoff, J. S.; Collard, D. M. *Macromolecules* **1999**, *32*, 4232−4239.
(46) Roncali, J.; Shi, L. H.; Garnier, F. *J. Phys. Chem.* **1991**, *95*, 8983−8989.
(47) El Kassmi, A.; Büchner, W.; Fache, F.; Lemaire, M. *J. Electroanal. Chem.* **1992**, *326*, 357−362.
(48) Büchner, W.; Garreau, R.; Lemaire, M.; Roncali, J.; Garnier, F. *J. Electroanal. Chem.* **1990**, *277*, 355−358.
(49) Shimizu, R. N.; Demarquette, N. R. *J. Appl. Polym. Sci.* **2000**, *76*, 1831−1845.
(50) Żenkiewicz, M. *JAMME* **2007**, *24*, 137−145.
(51) Bao, Z.; Lovinger, A. J. *Chem. Mater.* **1999**, *11*, 2607−2612.
(52) Hong, X. M.; Tyson, J. C.; Collard, D. M. *Macromolecules* **2000**, *33*, 3502−3504.
(53) Wang, B.; Watt, S.; Hong, M.; Domercq, B.; Sun, R.; Kippelen, B.; Collard, D. M. *Macromolecules* **2008**, *41*, 5156−5165.

DOI: 10.1021/acsmacrolett.5b00328
ACS Macro Lett. 2015, 4, 725−730